www.czasopisma.pan.pl PAN POLSKA AKADEMIA NAUK www.journals.pan.pl

A R C H I V E S O F M E T A L L U R G Y A N D M A T E R I A L S

Volume 60 2015 Issue 4

DOI: 10.1515/amm-2015-0485

Ł. POLOCZEK*, B. DYBOWSKI*,#, K. RODAK*, R. JAROSZ**, A. KIEŁBUS*

INFLUENCE OF AGE HARDENING PARAMETERS ON THE MICROSTRUCTURE AND PROPERTIES OF THE AlSi7Mg SAND CAST ALLOY

WPŁYW PARAMETRÓW UTWARDZANIA WYDZIELENIOWEGO NA STRUKTURĘ I WŁAŚCIWOŚCI STOPU AlSi7Mg

Aluminium alloys are characterized by a low density, acceptable mechanical properties and good technological properties. This unique connection of features made aluminium alloys perfect structural material for the transportation industry. Also, due to their good electrical conductivity they also found application in energy production industry. High mechanical properties and electrical conductivity of the Al-Si alloys with Mg addition may be achieved by heat treatment. However, the highest mechanical properties are achieved in the early stages of age hardening – due to precipitation of coherent phases, while high electrical conductivity may be achieved only by prolonged aging, during precipitation of semi-coherent or fully noncoherent, coarse phases. Carefully heat treated AlSi7Mg alloy may exhibit both fairly high electrical conductivity and slightly increased mechanical properties. The following article present results of the research of influence of heat treatment on the properties and microstructure of sand cast AlSi7Mg alloy. Microstructure observations were performed using light microscopy, scanning electron and scanning-transmission electron microscopy. Hardness and electrical conductivity of the AlSi7Mg alloy were investigated both in as-cast condition and after heat treatment. Maximum hardness of the alloy is achieved after solutioning at 540°C for 8h, followed by 72h of aging at 150°C, while maximal electrical conductivity after solutioning at 540°C for 48h, followed by 96h of aging at 180°C. Increase of the electrical conductivity is attributed to increasing distance between Si crystals and precipitation of semi coherent phases.

Keywords: AlSi7Mg, Sand casting, Microstructure, Electrical conductivity, Hardness, Heat treatment

Stopy aluminium charakteryzują się małą gęstością, dobrymi właściwościami mechanicznymi, a przy tym bardzo dobrymi właściwościami odlewniczymi. Połączenie tych cech powoduje że stopy te znajdują szerokie zastosowanie w przemyśle motoryzacyjnym. Ich dużą zaletą jest również wysoka przewodność elektryczna oraz cieplna, dzięki której znajdują również zastosowanie w przemyśle energetycznym. Uzyskanie tak wysokich właściwości mechanicznych i przewodności elektrycznej w przypadku stopów Al-Si z dodatkiem Mg może być osiągnięte tylko poprzez przeprowadzenie obróbki cieplenj. Najwyższe właściwości mechaniczne są osiągane w początkowej fazie utwardzania wydzieleniowego (wydzielanie się koherentnych faz), podczas gdy uzyskanie wysokich wartości przewodności może być osiągnięte tylko przez długotrwałe starzenie, podczas wydzielania się pół koherentnych lub niekoherentnych, dużych faz. W przypadku stopu AlSi7Mg, starannie dobrana obróbka cieplna może powodować znaczne podwyższenie przewodności oraz polepszenie właściwości mechanicznych. Ninjiejszy artykuł przedstawia wyniki badań wpływu parametrów obróbki cieplnej na strukturę i właściwości stopu AlSi7Mg, odlanego grawitacyjnie do form piaskowych. Obserwacje mikrostruktury prowadzone były prz użyciu metod mikroskopii świetlnej, elektronowej mikroskopii skaningowej oraz elektronowej mikroskopii transmisyjnej. Twardość i przewodności stopu AlSi7Mg badano zarówno w stanie lanym, jak i po obróbce cieplnej. Maksymalną twardość stopu uzyskano po przesycaniu w 540°C przez 8h oraz starzeniu w temperaturze 150°C przez 72h. Maksymalną przewodność elektryczną uzyskano po przesycaniu w 540° C przez 48h, oraz starzeniem w temperaturze 180°C przez 96h. Wzrost przewodności elektrycznej spowodowany jest zwiększeniem się odległości pomiędzy kryształami Si oraz wydzielaniem się półkoherentnych faz.

1. Introduction

Aluminium alloys are known for their low density and acceptable mechanical properties. Moreover, they exhibit good corrosion resistance and good technological properties. Unique combination of these properties made them perfect structural material for transportation industry [1÷3]. However, not only automotive or aerospace industries are interested in aluminium alloys. As aluminium is also a good electrical conductor, its alloys found application also in energy production industry. Some components, such as housings of gas insulated switchgears are produced from aluminium-silicon alloys. As these elements are large-sized and complex, they are mainly sand cast. The switchgears are insulated with SF_6 gas, so

* SILESIAN UNIVERSITY OF TECHNOLOGY, FACULTY OF MATERIAL SCIENCE AND METALLURGY, 8 KRASIŃSKIEGO STR., 40-019 KATOWICE, POLAND

** ZM "WSK RZESZÓW", 35-078 RZESZÓW, 120 HETMAŃSKA STR., POLAND

Corresponding author: bartlomiej.dybowski@polsl.pl

they need to be perfectly air-tight. The insulator is introduced into the switchgear under high pressure, so the material is exposed to static loads. In case of emergency (power surges etc.), high electrical conductivity of the alloy is required. Al-Si alloys seem to be perfect material for this application. High demanded properties may be achieved only after the age hardening treatment. Magnesium addition to the Al-Si alloys enables their heat treatment.

Age hardening leads to increase of both mechanical properties of the alloys as well as their electrical conductivity[4]. However, the peak hardness is exhibited by the alloy during the precipitation of fine, coherent with the matrix phases, while the highest electrical conductivity is attributed to the precipitation of coarse, incoherent phases. Carefully performed heat treatment may lead to formation of micro- and substructure which will assure high electrical conductivity without big drop of hardness of the alloy.

Al-Mg-Si and Al-Si-Mg alloys have been extensively investigated before. Despite many researches considered the precipitation sequences and phase transformation during the aging of the alloys, the results often are ambiguous[3], [5÷17]. The overall precipitation sequence in the Al-Mg-Si alloys is accepted to be [18]:

$$SSSS \rightarrow GP\ zones \rightarrow \beta'' \rightarrow \beta' \rightarrow \beta \qquad (1)$$

In fact, this sequence is much more complex. Depending of the alloy composition (balanced – in which Mg:Si atomic ratio is equal 2:1, excess of Mg, excess of Si), variety of GP zones and metastable phases is formed. The more complex proposed generic sequence is given[19]:

$$SSSS \rightarrow GP\ zones \rightarrow pre\ \beta \rightarrow \beta(Mg_5Si_6) \rightarrow \{U1, U2, B', \beta'\} \rightarrow \beta(Mg_2Si) \qquad (2)$$

Doan et. al. [5] summarised observed phases in each kind of alloy. The proposed sequences are shown in the table 1. β'' phase is coherent phase, with composition accepted to be Mg_5Si_7 [6, 9, 11, 13, 16], attributed to maximal strengthening effect. β' (Mg_2Si), Type A ($MgAl_2Si_2$) and Type B (MgAlSi) are metastable semi-coherent phases. Type A and Type B are most probably the same as U1 and U2 mentioned in the equation (2), however, their chemical compositions are varying [5, 8, 11, 12]. This ambiguity may be however caused by constant migration of atoms in the elevated temperature. Doan et al. [5] revealed that Type A and Type B (U1, U2) phases are observed only in the alloys with excess of Si, while Matsuda et al. [8] reported that Type B phase is observed in balanced alloy, replacing β' phase observed in the alloy with excess of Mg. Cuboid β (Mg_2Si), plate-like β (Mg_2Si) and Si are the only stable phases.

The commercial casting Al-Si alloys exhibit high excess of Si. According to Matsuda et al. [8] with increasing excess of Si, number of Type A, B and C (third one metastable phase, similar to B') increases, while number of β' phases decrease. Moreover, van Huis et al. [19] found that in the alloys with excess of Si, Type A phase is formed rather than Type B and B'. Coexistence of intermediate and stable phases – β'', Type A as well as Si is caused by a few factors. First of all, Type A phase is formed in the in situ transformations from β'' and pre- β'' phases [5]. As the phases formed in subsequent transformations contain less Si in the structure, the excess of it has to migrate somewhere [11]. Ravi et al. [11] found that Type A phase is more energetically favourable, so it is formed before the pure Si. Pure Si is more favourable only in the last stages of precipitation, during the β-Mg_2Si phase formation. Many other researchers found that the Type A phase and Si coexist during whole precipitation sequence.

Following article present results of the research on the microstructural changes during the solutioning and aging of the commercial AlSi7Mg casting alloy. The hardness and

TABLE 1

Precipitation sequences in Al-Si-Mg alloys, proposed by Doan et al [5].

Alloy	Temp [°C]	Ageing time [h] (0.1 / 1 / 10 / 100 / 1000)				
Excess Si	185	β''				β'', cuboid β
	210	β''		β'', cuboid β		β'', cuboid β, β'
	245	β''		β'', cuboid β		β'', cuboid β, β'
	300	cuboid β				-
	350	cuboid β				-
Quasi-binary	185	β''				β'', cuboid β
	210	β''		β'', cuboid β		β'', cuboid β, β'
	245	β''		β'', cuboid β		β', β
	300	β'', cuboid β		cuboid β, β', β		
	350	β'', cuboid β	cuboid β, β'		β'', cuboid β	
Excess Si	185	β''				
	210	β''	β'', Si		β'', Si, Type A	Si, Type A
	245	β''		β'', Si	β'', Si, Type A	Si, Type A
	300	β'', Type A, Type B	Si, Type A, Type B		β', Type A, Si	β, cuboid β, Si
	350	Si, Type A, Type B, β'		β, cuboid β, Si		

electrical conductivity of the alloy has been examined both in as cast condition and after heat treatment.

2. Research material and methodology

Investigated material was AlSi7Mg aluminium casting alloy. The chemical composition of the alloys is shown in the table 2. The alloy was sand cast in form of rods with diameter Ø=20mm and length l=120mm.

TABLE 2
Chemical composition of the AlSi7Mg alloy (wt. %).

Si	Mg	Mn	Fe	Ti	Na	Sr	Al
6.96	0.34	0.003	0.11	0.11	0.0078	0.0004	rest

The alloy was investigated both in the as-cast condition and after heat treatment. The rods were cut into the 5mm thick specimens, which were then solutioned at 535±5°C for 4-72h, followed by water cooling. The specimens were aged at 150±5°C and 180±5°C for 0.5-120h, followed by air cooling. Heat treatment was conducted in the resistance furnaces in air atmosphere.

The alloy microstructure was investigated by means of light microscopy (LM) on Olympus GX71 and Neophot 32 LM, scanning electron microscopy (SEM) on Hitachi S3400N SEM and scanning transmission electron microscopy (STEM) on Hitachi HD-2300A STEM. Specimens for LM and SEM observations were grinded on SiC abrasive papers (grades 80-1200) and polished on diamond suspensions with mean grain size 6-1μm. Final polishing step was done on colloidal silica with grain size 0.05μm. Observations were done on un-etched specimens. STEM specimens were electro-polished on TenuPol-5 electropolisher in solution consisting of 20% of nitric acid in methanol. Chemical composition of the phases observed in the structure was investigated by energy dispersive spectrometry (EDS) with detectors attached to SEM and STEM microscopes.

Electrical conductivity of the alloy was investigated by an eddy-current tester Sigmatest 2.069 with measuring range from 0.5 to 65 MS/m. Eight measurements were done on each specimen.

AlSi7Mg alloy hardness was measured by Brinell method on Rockwell-Brinell 15002P tester. The measurement were done with 5mm indenter, with load 250kg and indenting time equal 35s. Seven measurements were done on each specimen.

3. Research results

3.1. As cast microstructure

Previous investigations [20] revealed that AlSi7Mg alloy microstructure consists of α-Al solid solution dendrites and binary eutectic mixture α-Al + β-Si in the interdendritic regions. There are also observed intermetallic phases such as α-Al_{17}(Fe, Mn)$_3Si_2$, β-Al_5FeSi, π-$Al_9FeMg_3Si_5$ and Mg_2Si. These phases are formed in complex eutectic reactions during solidification. The quantitative parameters of the AlSi7Mg alloy microstructure in the as-cast conditions are given in table 3.

Fine precipitates are observed in the alloy in as-cast condition also within the dendrites. They posses globular or rod-like morphology. These are metastable Al-Si-Mg phases (U1, U2 etc.) and most probably β-Si crystals (Fig.1).

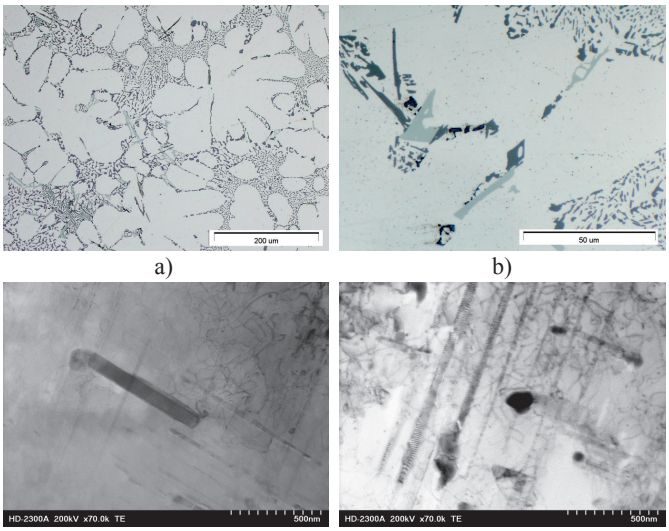

a) b) c) d)

Fig. 1. Microstructure of AlSi7Mg alloy in the as-cast condition; a, b) LM; c, d) STEM.

3.2. Microstructure after solutioning

Solutioning of the alloy leads to fragmentation of the eutectic silicon fibres. With increasing solution treatment time, the interdendritic silicon crystals coagulate and spheroidize (Fig. 2a). Quantitative evaluation of the interdendritic Si crystal revealed, that with increasing solutioning time, their mean area of the flat section increases (Fig. 3a), so the distance between the crystals does (Fig. 3b). Volume

TABLE 3
Quantitative parameters of the AlSi7Mg alloy microstructure in as-cast condition.

Phase	Volume fraction V[%]	Variability factor [%]	Mean area of the flat section $\bar{A}$ [μm^2]	Variability factor [%]	Distance between neighbours l [μm]	Variability factor [%]
Eutectic Si	8.9	22.4	4.5	188.9	3.1	58.9
Eutectic mixture	24.5	14.1	2063.0	475.0	45.7	63.0
Fe-bearing phases	0.62	37.6	16.9	127.0	15.3	109.0
Mg_2Si	0.03	285	2.05	125.0	127.0	22.0

fraction of the crystals does not change, it stays at the level of 8-9% (Fig. 3c). Mg_2Si phase dissolves within the matrix completely. π-$Al_9FeMg_3Si_5$ phase undergoes decomposition. Magnesium and excess of silicon dissolves in the matrix. The remaining elements are bonded in the forming new β-Al_5FeSi phase (Fig. 2b).

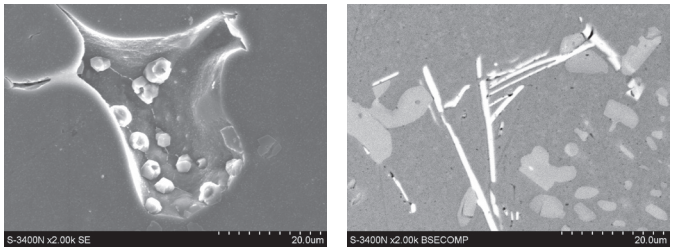

a) b)

Fig. 2. AlSi7Mg alloy microstructure after solution treatment, SEM; a) spheroidized Si crystals; b) β-Al_5FeSi formed after π phase decomposition.

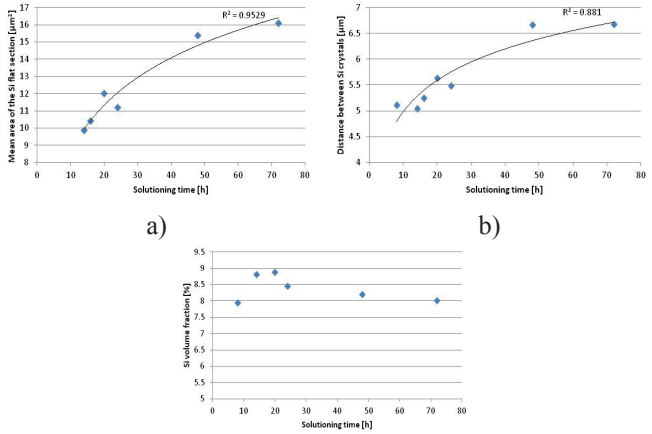

a) b)

c)

Fig. 3. Quantitative parameters of the interdendritic Si crystals after solutioning; a) Mean area of the Si flat section; b) Distance between Si crystals; c) Si volume fraction.

Fine precipitates, observed within the α-Al dendrites in the as-cast condition, dissolved during solution treatment. The only phases observed after in the solutioned specimens are fine rods or needles, rich in Al, Si and Ti (Fig. 4). These may be phases formed during the heat treatment or phases which were not dissolved.

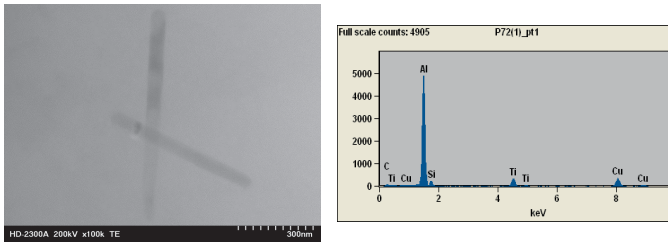

a) b)

Fig. 4. Fine phases within the α-Al dendrites after solution treatment, STEM; a) Rod- or needle like precipitates; b) corresponding EDS chart (Cu from the handle).

3.3. Microstructure after aging

Phases present in the interdendritic spaces do not undergo further transformations during ageing treatment. Their volume fraction as well as mean area of flat section is the same both after shortest aging and the longest one. Two processes are proceeding within α-Al dendrites. First one – precipitation and growth of fine needle- or plate-like phases. After six hours of aging at 180°C, many fine precipitates are observed (Fig. 5a). They are enriched in Mg, Si and probably Al (Fig. 5c). After 96 hours of aging, the needles grew in a significant way (Fig. 5b). Simultaneously, more coarse, equiaxed phases are formed (Fig. 6a, b). These phases are enriched especially in silicon (Fig. 6c), however, there are also observed phases with a slight content of magnesium (Fig. 6.d). With increasing aging time, number and size of these precipitates increase (Fig. 6b). Al-Si-Ti phases observed after solutioning are still present in the structure (Fig. 7)

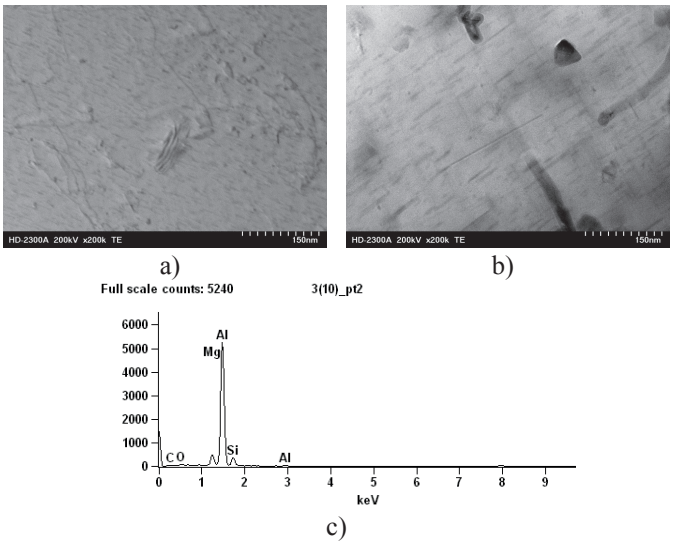

a) b)

c)

Fig 5. Fine needle- or plate-like precipitates within the α-Al dendrites, STEM; a) after 6h of aging at 180°C; b) after 94h of aging at 180°C; c) EDS spectrum from these phases.

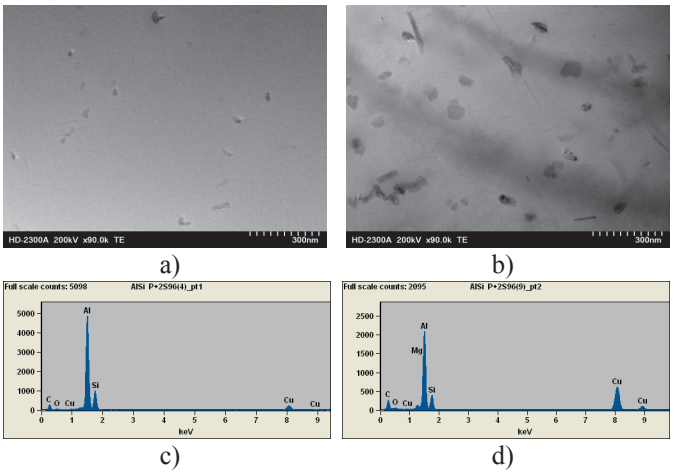

a) b)

c) d)

Fig. 6. Equiaxed phases within the α-Al dendrites, STEM; a) after 6h of aging at 180°C; b) after 94h of aging at 180°C; c, d) EDS spectra from these phases (Cu from the handle).

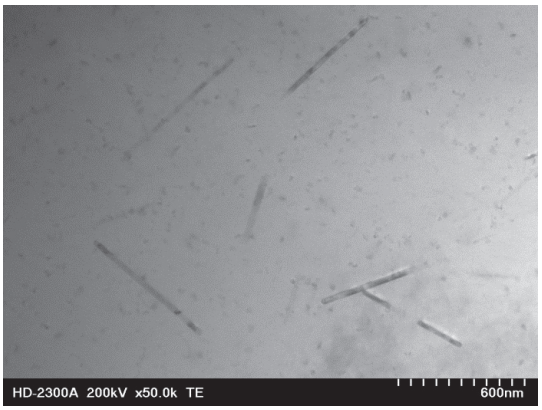

Fig. 7. Coarse needle- or plate-like phases containing Al, Si and Ti in the AlSi7Mg alloy after aging; a) 10h of aging at 180°C.

3.4. AlSi7Mg alloy properties

AlSi7Mg alloy hardness in as-cast condition is equal 62±3HB, while its electrical conductivity is equal 22.2±0.5 MS/m. After solution treatment, the hardness increasedup to 75±4HB after 48h of solutioning at 535°C (Fig. 8a). The electrical conductivity decreased to the level of 21.5±0.1 MS/m. It seems that with increasing solutioning time, the conductivity slightly increases (Fig. 8b).

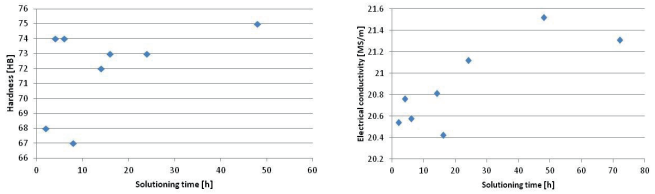

a) b)

Fig. 8. AlSi7Mg alloy properties after solutioning for different times; a) Hardness; b) Electrical conductivity.

Aging at 150°C of the AlSi7Mg alloy solutioned for 8 hours led to increase of the hardness up to 106±2HB after 72h (Fig. 9a). Aging at 180°C of the alloy led to increase of hardness up to 103±3HB after 6 hours of aging (Fig. 10a). The electrical conductivity increased up to 23.7±0.2 MS/m after 120h of aging at 150°C (Fig. 9b) and increased even further up to 25.2±0.1 after aging for 120h at 180°C (Fig. 10b). Aging at 180°C of the alloy solutioned for 48h led to achievement of hardness at the level of 101±3 HB after 10h of aging (Fig. 11a). The electrical conductivity of the alloy solutioned for 48h increased up to 26.6±0.1 MS/m after aging for 96h (Fig. 11b).

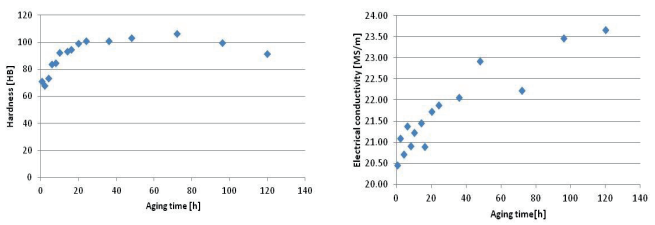

a) b)

Fig. 9. AlSi7Mg alloy properties after aging at 150°C for different times; a) Hardness; b) Electrical conductivity.

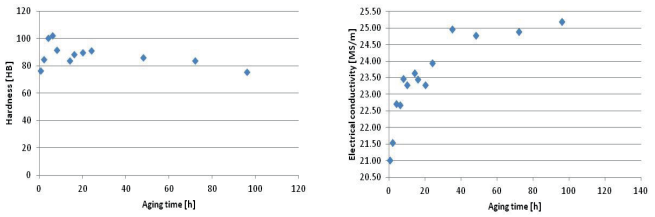

a) b)

Fig. 10. AlSi7Mg alloy properties after aging at 180°C for different times; a) Hardness; b) Electrical conductivity.

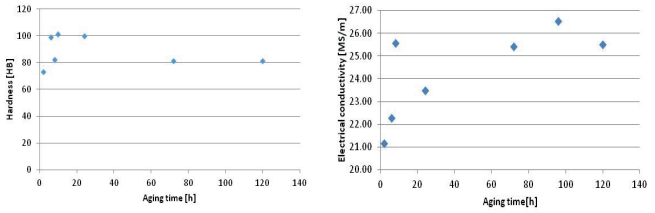

a) b)

Fig. 11. Solutioned for 48h AlSi7Mg alloy properties after aging at 180°C for different times; a) Hardness; b) Electrical conductivity.

4. Discussion

AlSi7Mg alloy microstructure in the as-cast condition consist of α-Al solid solution dendrites and α-Al+β-Si binary eutectic mixture. During the solidification process intermetallic phases such as α-$Al_{17}(Fe, Mn)_3Si_2$, β-Al_5FeSi, π-$Al_9FeMg_3Si_5$ and Mg_2Si are also formed in more complex eutectic reactions. As previous investigations shown, there are observed also fine, non-equilibrium phases within the α-Al dendrites. These phases are most probably formed as a secondary precipitates, formed after complete solidification of the alloy. As the sand casting is characterized by a slow cooling rates, the alloy is exhibited for an elevated temperature for a relatively long time. Some aging processes may take place during this time. Hardness of the alloy in as cast condition is equal 62±3HB, while its electrical conductivity is equal about 22.2±0.5 MS/m.

Solutioning of the alloy leads to fragmentation, coagulation and spheroidization of eutectic Si crystals. However, there were not observed any considerable changes in its volume fraction. With increasing solutioning time, mean area of the Si crystal increased. Distance between the closest neighbours also increased. It indicates, that the diffusion processes take place during the solutioning, however they do not lead to further dissolution of the eutectic Si. Mg_2Si phase on the other hand is being dissolute completely. π-$Al_9FeMg_3Si_5$ phase also undergoes dissolution. After the shortest times of the solutioning, the phase is partially dissolved in the matrix (Fig. 12a). Mg and excess of Si are dissolute within the matrix, while rest of elements is bounded in newly formed β-Al_5FeSi phase (Fig. 12b). After prolonged solutioning, whole π-phase is dissoluted. Fine precipitates within the α-Al dendrites are dissoluted after solution heat treatment. Only the needles or plates of Al-Ti-Si rich phase are observed within the dendrites after solutioning. The hardness of the AlSi7Mg increases after solution treatment. It is probably caused by a slight solid solution hardening by soluted alloying elements. As the volume fraction of the brittle intermetallic phases did

not decreased significantly – the hardening mechanism by secondary phases should not be affected. The considerable decrease in the alloy electrical conductivity also suggest this mechanism. The presence of the alloying elements in the matrix crystal structure increases resistivity of the alloy. Slight increase in electrical conductivity of the alloy after the longest solutioning time is probably attributed to increasing distance between closest Si crystals. Aluminium is characterized by a considerably lower resistivity than Si, so it can be assumed, that the electricity will be conducted by the Al dendrites. Each Si particle act as a obstacle, so higher distance between them will enhance the conductivity.

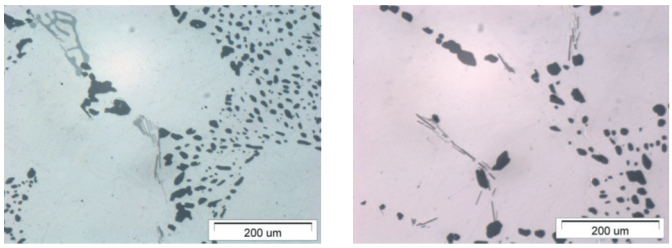

a) b)

Fig. 12. Degradation of π-$Al_9FeMg_3Si_5$ during the solutioning of the alloy, LM; a) 4h of solutioning at 535°C; b) 48h of solutioning at 535°C.

During the aging process two phenomena are occurring simultaneously within the α-Al dendrites. Firstly, fine needle- or plate-like phases are formed and grow during the ongoing ageing. The phases are enriched in Mg, Si and most probably Al. Second process is formation and growth of more coarse, equiaxed phases, rich in silicon. After the longest ageing times number and size of these particles increase. As EDS investigations revealed, these phases contain mainly Si and perhaps Al. As there are no equilibrium and non-equilibrium phases in Al-Si system, they are perhaps fine Si particles. This is in agreement with available literature. As the subsequently formed phases are continuously depleted in the Si, its excess is precipitated in form of fine Si crystals. Part of the equiaxed precipitates are most probably transvers sections of needle- or rodlike phases. Froseth et al [6] found that fine β" precipitates are characterized by length equal to about 30-40nm, while U1 and U2 phases length ranges from 50nm up to several hundreds of nm. The stable Mg_2Si has a platelet-like morphology and has dimensions up to several microns. In our research we have found that after 6 hours of aging at 180°C, length of the precipitates is equal about 25nm, which may indicate presence of β" phase. Peak hardness of the alloy is observed during precipitation of these phases, which may confirm the presence of β" phase. After prolonged aging for 96h at 180°C, length of precipitates increased up to about 80-100nm, which indicates presence of semi-coherent U1 phases. The diameters are slightly smaller than these, reported in literature, however, it is in good agreement with Gupta et al. [3], who found that excess of Si refines the structure. Presence of U1 phase after aging at 180°C is not in agreement with Doan et al. [5] who stayed that at this temperature only β" is formed. However, AlSi7Mg alloy was investigated in our research. The excess of Si in this alloy is very high, which may lead to former presence of U1 phase.

Hardness of the AlSi7Mg alloy is the highest after 72h of aging at 150°C and is equal 106±2HB. At 180°C the peak hardness is noticed after 6hours of aging and is equal 103±3HB. The electrical conductivity increases both with increasing aging time and aging temperature. At standard solutioning parameters (8h/535°C), maximal achieved conductivity is equal 25.2±0.1 MS/m after 96h of aging at 180°C. Increase of conductivity after aging is caused by bounding of soluted in α-Al elements in the intermetallic phases. As the phases change morphology and grow (smaller area of phase boundaries) with increasing aging time and temperature, the conductivity considerably increase. Further increase up to 26.6±0.1 MS/m is achieved after aging of the alloy with applied prolonged solutioning (48h). What is important, prolonged aging did not lead to decrease in hardness of the alloy (101±3 HB after 10h of aging at 180°C).

5. Conclusions

Solutioning of the AlSi7Mg alloy at 535°C leads to fragmentation and coagulation of eutectic Si crystals. Prolonged solutioning time leads to increase of Si crystal flat section area and distance between closest precipitates.

Aging of the AlSi7Mg alloy leads to formation of fine needle- or plate-like phases, rich in Al, Si and Mg. With increasing time, the phases grow. Simultaneously, more coarse, equiaxed phases rich in Si are formed.

Electrical conductivity of the AlSi7Mg alloy decreases after solutioning at 535°C, which is attributed to alloying elements atoms soluted in the α-Al crystal structure. Following aging leads to considerable increase of the conductivity by bonding of the elements in the less harmful intermetallic phases.

Prolonged solutioning time causes further increase of the electrical conductivity of the AlSi7Mg alloy. It is caused by increasing distances between Si crystals. Prolonged solutioning time does not affects hardness of the alloy.

Acknowledgments

The present work was supported by the Polish National Centre for Research and Development under the research project No PBS2/B5/28/2013.

REFERENCES

[1] K. Li, M. Song, Y. Du, X. Fang, Arch. Metall. Mater. **57**, 2 (2012).
[2] Š. Eperješi, M. Matvija, Ľ. Eperješi, M. Vojtko, Arch. Metall. Mater. **59** (2014).
[3] AK. Gupta, D.J. Lloyd, S.A. Court, Mater. Sci. Eng. A **316,** 11–17 (2001).
[4] A. Hossain, A.S. W. Kurny **4**, 288–293 (2014).
[5] L.C. Doan, K. Nakai, Y. Matsuura, S. Kobayashi, Y. Ohmori, Mater. Trans. **43**, 6, 1371–1380 (2002).
[6] G. Froseth, R. Hoier, P.M. Derlet, S.J. Andersen, C.D. Marioara, Phys. Rev. B **67**, 1- 11 (2003).
[7] K. Teichmann, C.D. Marioara, S.J. Andersen, K. Marthinsen,

Mater. Charact. **75**, 1–7, (2013).
[8] K. Matsuda, S. Ikeno, K. Terayama, H. Matsui, T. Sato, Y. Uetani, Metall. Mater. Trans. A **36**, 2007–2012 (2005).
[9] H. W. Zandbergen, Science **277**, 5330, 1221–1225 (1997).
[10] N. Afify, a. Gaber, M. S. Mostafa, G. Abbady, J. Alloys Compd **462,** 80–87 (2008).
[11] C. Ravi, Acta Mater. **52**, 14, 4213–4227 (2004).
[12] S.J. Andersen, C.D. Marioara, a. Frøseth, R. Vissers, H.W. Zandbergen, Mater. Sci. Eng. A **390**, 1–2, 127–138 (2005).
[13] S.J. Andersen, H.W. Zandbergen, J. Jansen, C. TrÆholt, U. Tundal, O. Reiso, Acta Mater. 46, 9, 3283–3298 (1998).
[14] G.A. Edwards, K. Stiller, G.L. Dunlop, M.J. Couper, Acta Mater. **46**, 11, 3893–3904 (1998).
[15] S.J. Andersen, C.D. Marioara, R. Vissers, a. Frøseth, H.W. Zandbergen, Mater. Sci. Eng. A **444**, 1–2, 157–169 (2007).
[16] T. Epicier, F. Bosselet, J.C. Viala, Interface Sci. **1**, 213 (1994).
[17] [W. Miao, D. Laughlin, Scr. Mater. **40,** 7, 873–878 (1999).
[18] H. Liao, Y. Wu, K. Ding, Mater. Sci. Eng. A **560**, 811–816 (2013).
[19] D.J. Chakrabarti, Y. Peng, D.E. Laughlin, Mater. Sci. Forum **396–402,** 857–862 (2002).
[20] M. a. van Huis, J.H. Chen, H. W. Zandbergen, M.H.F. Sluiter, Acta Mater. **54**, 11, 2945–2955 (2006).
[21] B. Dybowski, B. Adamczyk-Cieślak, K. Rodak, I. Bednarczyk, A. Kiełbus, J. Mizera, Solid State Phenomena **229,** 3-10 (2015).

Received: 20 November 2014.